

# Mechanistic Similarities between 3D Human Bronchial Epithelium and Mice Lung, Exposed to Copper Oxide Nanoparticles, Support Non-Animal Methods for Hazard Assessment

Joseph Ndika, Marit Ilves, Ingeborg M. Kooter, Mariska Gröllers-Mulderij, Evert Duistermaat, Peter C. Tromp, Frieke Kuper, Pia Kinaret, Dario Greco, Piia Karisola, and Harri Alenius\*

The diversity and increasing prevalence of products derived from engineered nanomaterials (ENM), warrants implementation of non-animal approaches to health hazard assessment for ethical and practical reasons. Although non-animal approaches are becoming increasingly popular, there are almost no studies of side-by-side comparisons with traditional *in vivo* assays. Here, transcriptomics is used to investigate mechanistic similarities between healthy/asthmatic models of 3D air–liquid interface (ALI) cultures of donor-derived human bronchial epithelia cells, and mouse lung tissue, following exposure to copper oxide ENM. Only 19% of mouse lung genes with human orthologues are not expressed in the human 3D ALI model. Despite differences in taxonomy and cellular complexity between the systems, a core subset of matching genes cluster mouse and human samples strictly based on ENM dose (exposure severity). Overlapping gene orthologue pairs are highly enriched for innate immune functions, suggesting an important and maybe underestimated role of epithelial cells. In conclusion, 3D ALI models based on epithelial cells, are primed to bridge the gap between traditional 2D *in vitro* assays and animal models of airway exposure, and transcriptomics appears to be a unifying dose metric that links *in vivo* and *in vitro* test systems.

## 1. Introduction

Nanotechnology has delivered innovative solutions for a broad range of industrial and consumer applications. However, as the field develops and new products continuously emerge, the likelihood of uncontrolled human exposure to engineered nanomaterials (ENM) is also growing. A large part of ENM hazard assessment has so far been carried out *in vivo* on a material-by-material basis. As a result of their durability, the chronic and systemic effects of nanoparticles are better studied in *in vivo* set-ups. However, taking the ever-increasing number and diversity of ENM into account, it is not feasible to test all these materials *in vivo* with regards to time, cost, and ethical considerations. Several ways to reduce and refine animal testing have been proposed but the ultimate goal is to replace animal experimentation with alternative methods.<sup>[1,2]</sup>

Dr. J. Ndika, Dr. M. Ilves, Dr. P. Karisola, Prof. H. Alenius  
Human Microbiome Research Program  
Faculty of Medicine  
University of Helsinki  
Helsinki 00290, Finland  
E-mail: harri.alenius@helsinki.fi, harri.alenius@ki.se  
Dr. I. M. Kooter, M. Gröllers-Mulderij, E. Duistermaat,  
P. C. Tromp, Dr. F. Kuper  
The Netherlands Organization for Applied Scientific  
Research TNO  
P.O. Box 80015, Utrecht 3584 CB, The Netherlands

Dr. P. Kinaret  
Institute of Biotechnology  
Helsinki Institute of Life Science  
University of Helsinki  
Helsinki 00790, Finland  
Prof. D. Greco  
Faculty of Medicine and Health Technology  
Tampere University  
Tampere FI-33014, Finland  
Prof. H. Alenius  
Institute of Environmental Medicine  
Karolinska Institutet  
P.O. Box 210, Stockholm SE-17176, Sweden

 The ORCID identification number(s) for the author(s) of this article can be found under <https://doi.org/10.1002/smll.202000527>.

© 2020 The Authors. Published by WILEY-VCH Verlag GmbH & Co. KGaA, Weinheim. This is an open access article under the terms of the Creative Commons Attribution License, which permits use, distribution and reproduction in any medium, provided the original work is properly cited.

DOI: 10.1002/smll.202000527

Possible alternative methods to *in vivo* testing span *in vitro* and *ex vivo* systems to *in silico* approaches.<sup>[3]</sup> Cell lines have been widely used for nanotoxicological testing and although they are easy and cheap to handle, these models have disadvantages such as being immortalized, having reduced differentiation ability and lack of individual variety, calling into question how adequately they represent cell behavior *in vivo*.<sup>[4]</sup> Primary cells are a better choice to reflect the actual cell behavior, but they in turn have limited life span, and similarly to cell lines, consist of only one cell type.<sup>[5]</sup> To overcome these shortcomings, advanced 3D *in vitro* systems consisting of polarized mucociliary differentiated airway epithelial cell layers, that more resembles the human airway epithelium (MucilAir), have been developed.<sup>[6]</sup> According to the manufacturer (Epithelix Sàrl, Switzerland), these primary cells can be cultured at an air–liquid interface (ALI) in a homeostatic state for more than a year. Another very significant limitation of traditional *in vitro* systems is that the majority of studies that are intended to mimic pulmonary exposures (for example, using cell lines or primary cells from respiratory tract), are conducted in submerged cell culture conditions, as opposed to direct exposure via air. The protein corona derived from serum in culture media alters the biological identity of the nanoparticles before they encounter the cells.<sup>[7]</sup> ALI models based on epithelial cells provide a possibility to mimic real-life aerosol exposure in order to investigate adverse events associated with inhaled ENM at the respiratory tract barrier.<sup>[8]</sup> Cells derived from individuals with lung pathologies such as asthma, allergic rhinitis, chronic obstructive pulmonary disease and cystic fibrosis (Epithelix Sàrl, Switzerland), have also been incorporated into this system. This is an important aspect of hazard assessment since the airway of individuals with prevalent pulmonary diseases, such as asthma, is more sensitive to ENM exposure.<sup>[9]</sup> Thus, the validation of such models as non-animal alternatives would add significant value to ENM safety evaluation.

Although the nanotoxicological community has heeded calls to take advantage of non-animal testing methods, side-by-side comparisons of traditional *in vivo* exposures with alternative testing systems are lacking. *In silico* methods that predict structure-activity interactions of ENM or focus on biomarker identification when used in tandem with experimental models, have become a promising approach of the 3R concept.<sup>[10]</sup> Therefore, in this study we use a systems level approach (microarray-based transcriptomics) to explore the comparability of ALI cultures based on donor-derived healthy and asthmatic human bronchial epithelial cells to traditional healthy and ovalbumin-induced mouse models of allergic airway inflammation, after exposure to pristine (CuO) or carboxylated (CuO<sup>COOH</sup>) copper oxide nanoparticles. With over 1700 publications in PubMed, 60% of which have been published in the last 10 years, copper oxide toxicity is clearly an area of significant interest.

## 2. Results

### 2.1. Exposing Healthy or Diseased Airways to Copper Oxide Nanoparticles Triggers Dose-Dependent Changes in Gene Expression *In Vivo* and *In Vitro*

Enhanced expression of IL33 (marker of allergic airway inflammation) as well as MUC5AC and MUC5B (mucus

hypersecretion) in asthmatic donor cells and inflamed lung tissue of mice, underscores a pre-existing asthmatic phenotype in both the *in vitro* and *in vivo* models without exposure to ENM (Figure 1A). As such, we here onward refer to the mice with OVA-induced allergic airway inflammation as asthmatic mice.

A dose-dependent response, characterized by the number of differentially expressed genes (DEG), was observed in mouse lung and human donor cells for each nanoparticle subtype (Figure 1B). On average, the highest and lowest number of DEG were observed in mouse lung and human donor cells exposed to high and low concentrations of nanoparticles respectively. The number of DEG did not clearly distinguish particle surface charge characteristics (pristine versus COOH-functionalized surface) and airway disease state (healthy versus asthmatic) in both mouse and human exposures, but a net decrease in number of DEG can be seen in asthmatic relative to healthy mouse lung tissue.

In order to investigate the underlying mechanisms of toxicity, gene set enrichment analysis was performed on pooled (low, mid and high concentration) DEG. This was followed by Venn comparisons of enriched biological processes in healthy and asthmatic airways exposed to either CuO or CuO<sup>COOH</sup> nanoparticles. Although several unique biological processes dissociating healthy/asthmatic and CuO/CuO<sup>COOH</sup> exposures were identified, the central overrepresented biological processes (response to cytokine, response to toxic substance, metal ion response, and response to oxidative stress) in both mouse and human exposures, are consistent on adverse exposure to partially soluble metal oxide-based nanoparticles (Figure 1C).

### 2.2. Copper Oxide Nanoparticles Trigger Common DEG in Mouse Lung and Human ALI Model

Because of the pathway-level similarities identified between mouse and human exposures, we next sought to identify overlapping DEG. From the perspective of alternative testing, *in vitro* testing systems will have added relevance if organ level DEG are similarly triggered *in vitro*.

18 591 human orthologues to mouse genes were downloaded from ENSEMBL. In this way mouse genes with corresponding human orthologues were compared with genes identified from ALI cultures of donor human bronchial epithelia. 12 252 genes were identified between mouse lung tissue and human bronchial epithelia, of which 1936 were differentially expressed in both mouse and human exposures (Figure 2A,B). These 1936 shared mouse and human DEG correspond to 30% and 31% of all the genes that were differentially expressed in response to CuO and CuO<sup>COOH</sup> nanomaterials in human bronchial epithelia and mouse lung tissue respectively. These 1936 genes, as well as their fold change in expression in both human and mouse exposures are provided as Table S1, Supporting Information.

Gene set enrichment analysis based on the shared mouse and human DEG, reveal that these genes are signature genes of human bronchial epithelial cells and human/mouse bulk lung tissue (Figure 2C, upper panel). The most significant biological processes represented by these shared genes are again consistent with known<sup>[11–16]</sup> pathobiological responses to metal oxide-based nanoparticles (Figure 2C, lower panel). These were; response to organic substance (adj. *p* value 1E-24 to 3E-28),

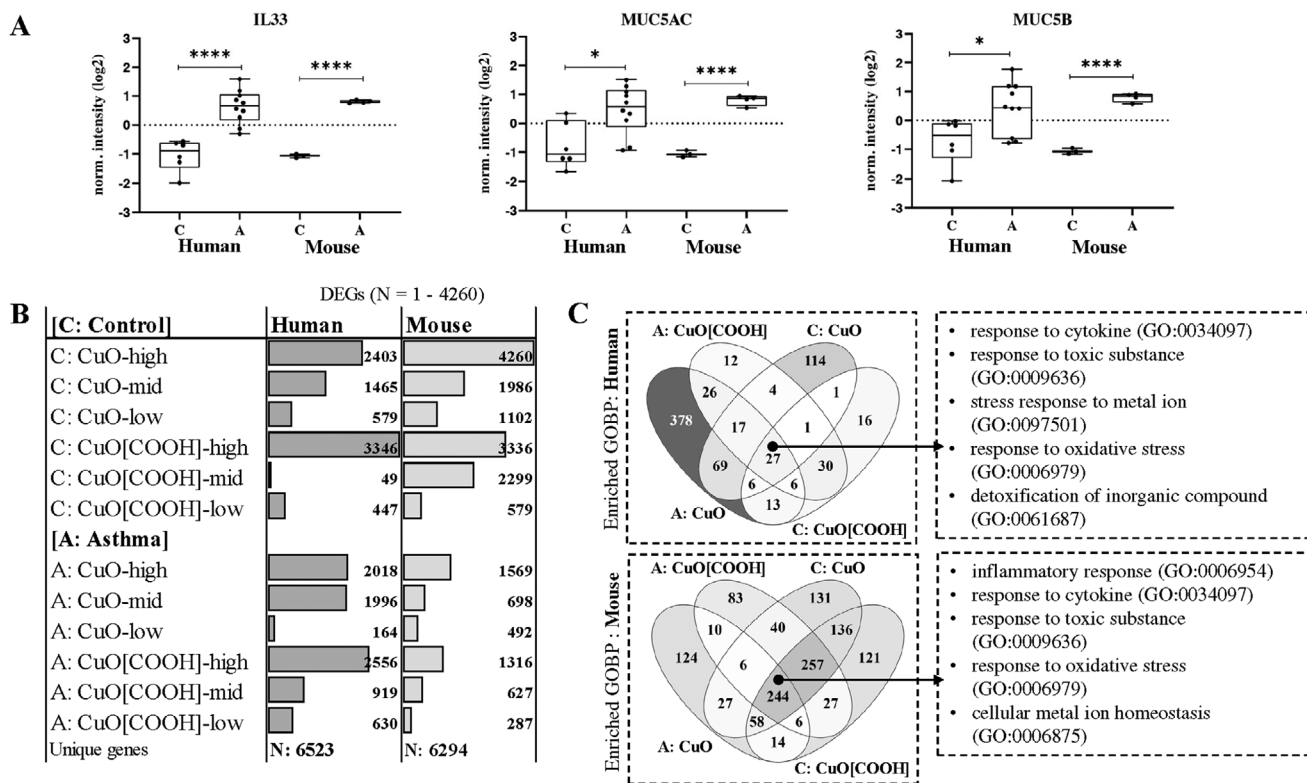


**Figure 1.** Mechanism of action-based health hazard assessment of pristine or COOH-functionalized copper oxide nanoparticles in healthy versus asthmatic airways. A) Selected signature genes distinguish control from inflamed (asthmatic) airways, in both mouse lung tissue and air-liquid interface cultures of human bronchial epithelial cells. Mouse tissue and human cells were exposed to three different concentrations of pristine (CuO) and COOH-functionalized (CuO [COOH]) copper oxide nanoparticles. B) Dose-dependent modulation of gene expression (number of differentially expressed genes) was observed in both mouse and human airways, in response to each nanoparticle type. C) Venn comparisons of enriched biological processes represented by corresponding differentially expressed genes, show material-specific responses as well as exposure-disease interaction. In human and mouse exposure models, biological processes directly related to metal-based nanoparticle exposure (oxidative stress, response to metal ion, etc.), were similarly triggered by both nanoparticle sub-types in healthy and inflamed airways.

response to stress (adj.  $p$  value  $2.1E-21$ ), regulation of cell death ( $3.2E-18$ ) and response to cytokine, metal ion, and oxidative stress (adj.  $p$  value  $3.3E-7-9.5E-18$ ). Several biological processes were enriched by genes that are uniquely differentially expressed in either the human or mouse exposures (Figure S1, Supporting Information). The DEG unique to mouse exposures were mainly involved in cell-mediated immune responses such as granulocyte activation and neutrophil mediated immunity, whilst those DEG that were unique to the human in vitro exposures are predominantly involved in microtubule-based processes such as ciliary transport and cilium organization. Nonetheless, almost half ( $[(17 + 81)/(52 + 52)]$ ) of the biological processes represented by mouse- or human-specific DEG were also identified amongst the biological processes from shared mouse and human DEG (Figure S1, Supporting Information).

### 2.3. Following Exposure to Copper Oxide Nanoparticles, Healthy Human and Mouse Airways have More DEG in Common than Asthmatic Human and Mouse Airways

We next asked whether the shared human and mouse DEG could also distinguish exposed healthy airways from exposed asthmatic airways. Shared DEG were separately compared for either healthy or asthmatic airways. More DEG were

shared between healthy (75%) human/mouse (1414 DEG) than between asthmatic (37%) human/mouse (605 DEG) exposures (Figure 3A,B).

Comparative functional enrichment analysis of shared DEG from asthmatic and healthy human and mouse airways, highlights differential response mechanisms that may reflect disease-related enhanced sensitivity of asthmatic airways to nanoparticle exposure. Whilst cellular response to chemical stimulus and response to organic substance were similarly enriched GO terms in healthy and asthmatic airways, notable differences are absence (decreased) of cilium movement, decreased response to stress, decreased response to oxidative stress, and enhanced cytokine and immune system processes in exposed asthmatic airways (Figure 3C,D).

### 2.4. Shared Mouse and Human DEG Incorporate Particle Dose and Enhanced Particle Sensitivity of Diseased Airways

Having observed an enrichment of biological processes relevant to general toxicant and also specific to metal oxide-based nanoparticle exposures, from the subset of shared human/mouse DEG, we next sought to answer whether these genes could categorize all samples according to particle sub-type, dose, or airway disease state.

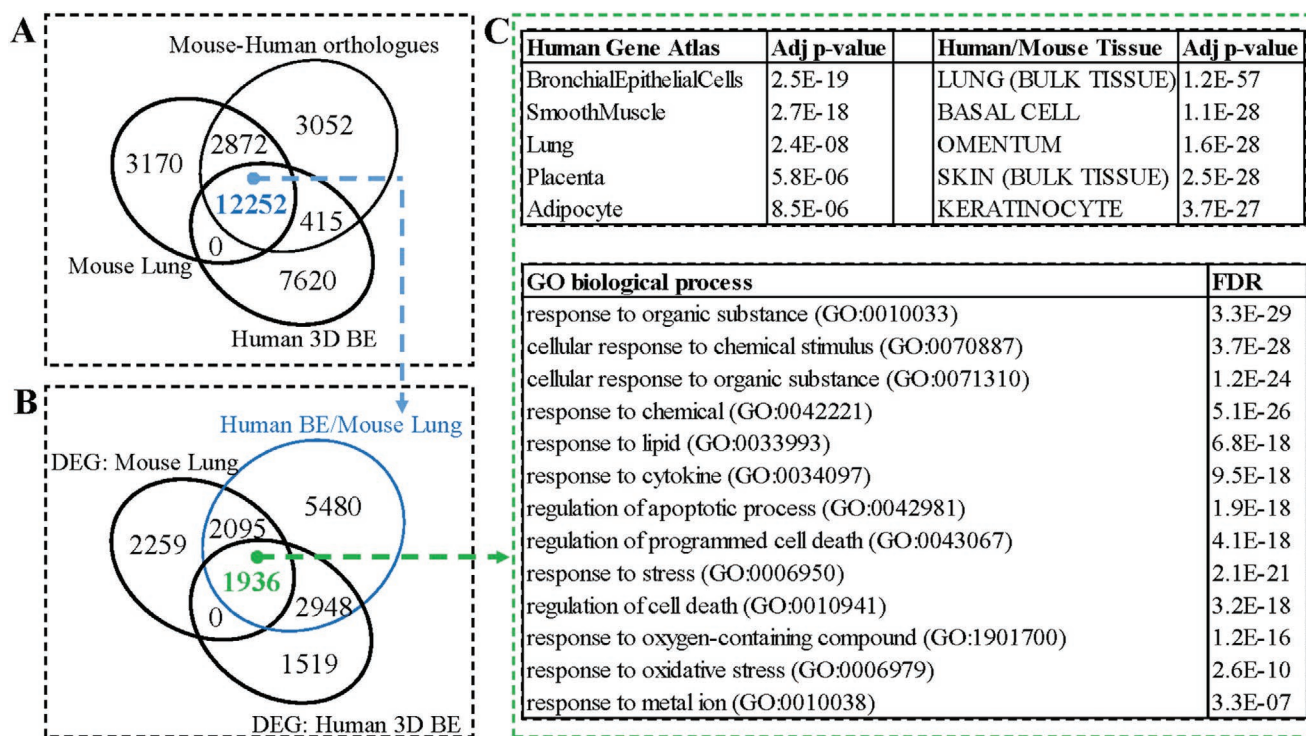


**Figure 2.** Orthologue-based comparisons of mouse lung tissue and human-derived bronchial epithelia transcriptomes. A) 18 591 human orthologues of mouse transcriptome were downloaded from ENSEMBL, of which 12 252 are expressed in an air-liquid interface model of human 3D bronchial epithelia. B) 1936 genes were triggered by exposure of mouse airway and human bronchial epithelia to at least one of three different doses for both CuO and CuO<sup>COOH</sup> nanoparticle exposures. C) Gene set enrichment analysis of these shared differentially expressed genes, reflects both the tissue and cell type origin of these genes (upper panel). The top-most enriched biological process is response to organic substance (GO:0010033). In fact, the top five functions represented by these genes all correspond to biological processes that are consistent with general cellular response to chemicals. Other top enriched functions are cytokine response, apoptosis, response to stress, oxidative stress, and metal ion response—all of which indicate adverse exposure to metal oxide-based nanoparticles (C; lower panel).

We performed principal component analyses based on the expression intensity of shared human and mouse DEG across all independent exposures. In healthy airways, the top two principal components, accounting for 53% of the total variation within the specified set of genes, grouped all exposures along a dose-response gradient in both human and mouse exposures (Figure 4, upper panel). In healthy airways, samples grouped according to; unexposed controls, low dose, mid dose, and high dose. In asthmatic airways, the top two principal components, explaining about 45% of the sample variance related to the specified subset of shared human and mouse genes, also grouped the exposures according to dose. But unlike in healthy airways, the low and mid doses clustered together in the mouse exposures, whilst the mid and high dose samples clustered together in the human exposures (Figure 4, lower panel and dotted squares). No clear separation of CuO- and CuO<sup>COOH</sup>-exposed samples could be seen in both human and mouse airways.

## 2.5. Cross Correlation Analysis Identifies Clusters of Highly Positively Correlated Genes with Functional Relevance to Adverse Nanoparticle Exposure

Because shared human and mouse DEG may not necessarily have the same direction of activation in human and mouse airways, we performed mouse-human correlation analysis based

on shared DEG. In healthy and asthmatic airways four sets of positively correlated ( $R > 0.8$ ) clusters were identified; #1: m1-H1 (114 shared genes) and #2: m2-H2 (70 shared genes) in asthmatic and #3: m3-H3 (458 shared genes), and #4: m4-H4 (269 shared genes) in healthy (Figure 5A,B). Enriched biological processes were only identified from the shared genes in clusters m1-H1 (asthmatic airways) and the shared genes in clusters m3-H3 (healthy airways). A Venn comparison of these biological processes, as well as a list of the top enriched biological processes, is depicted in Figure 5C.

## 2.6. Shared Upregulated as Opposed to Downregulated Genes Dictate Similarity and Specificity of Mouse and Human Airway Response to CuO Nanoparticles

Thus far a subset of genes that are, 1—commonly differentially expressed in exposed human and mouse airways, 2—highly positively correlated between human and mouse, and 3—enriched for biological functions that are consistent with adverse exposure to CuO and CuO<sup>COOH</sup> nanoparticles, have been identified in shared DEG from both healthy and asthmatic human and mouse airways (Figure 5C).

We next asked whether these subsets of genes represent a core transcriptomic signature that incorporates dose-response to copper oxide nanoparticles, irrespective of whether the target

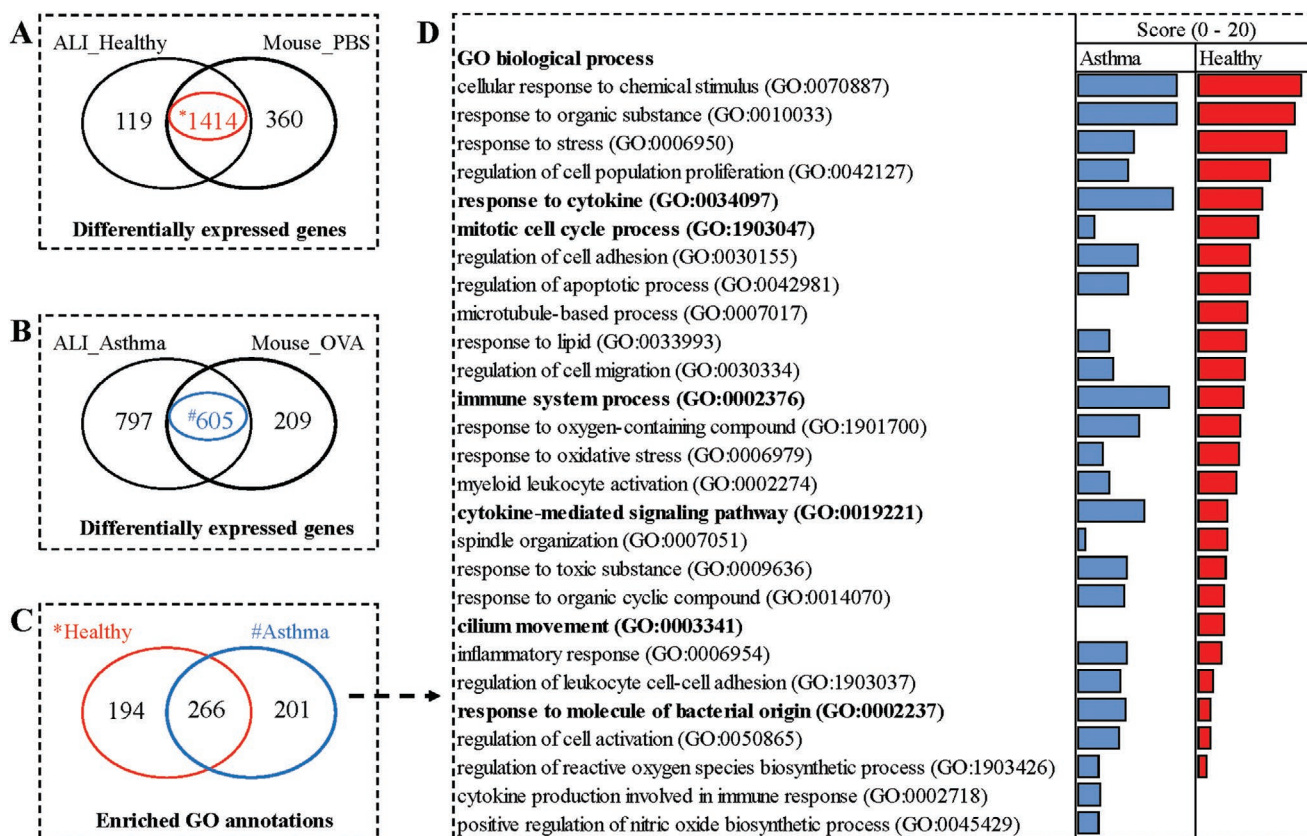


**Figure 3.** Mouse–human comparisons of number and functions of shared differentially expressed genes in A) control and B) asthmatic airways. Over two times more differentially expressed genes were commonly triggered in healthy (A) when compared to asthmatic (B) mouse and human airways. C) As expected, unique and shared over-represented biological processes were identified between the common mouse–human genes in healthy and asthmatic airways. Gene set enrichment analysis was carried out using the Panther tool, implemented within the Gene Ontology database. D) Top ranked biological processes, from shared mouse–human differentially expressed genes, for control and asthmatic airways are listed. The scale represents the score, calculated as the fold enrichment (cut-off, 1.5-fold) multiplied by the  $-\log$  of the false discovery rate (cut-off, 0.05). Each biological process represents a minimum of ten differentially expressed genes.

is human or mouse airway. Hierarchical clusters of both human and mouse samples were generated from the shared genes identified in each of the positively correlated mouse–human gene clusters (m1–H1, m2–H2, m3–H3, and m4–H4, depicted in Figure 5). The relative expression of each gene was obtained separately for human and mouse samples by Z-score normalization, and the average value from three to six biological replicates was used to generate the hierarchical clusters. Interestingly, clear dose-response hierarchical clusters emerged only from the shared genes between correlated clusters m1–H1 and m3–H3 (red boxes in Figure 5A,B, Figure 6, and Figure S2, Supporting Information). This is in line with the identification of significantly enriched biological processes—all of which were consistent with ENM exposure, only in the shared genes from these two sets of clusters (Figure 5C).

It was also notable that whilst all shared positively correlated DEG from clusters m1–H1 and m3–H3 are upregulated (Figure 6), the shared positively correlated DEG from clusters m2–H2 and m4–H4 are downregulated (Figure S2, Supporting Information). Human versus mouse correlation plots of three selected genes with functional relevance in regulation of oxidative stress (GLRX gene), response to metal ion (MT1F gene) and inflammatory response (IL6 gene), are shown in Figure 7.

### 3. Discussion

Several alternative testing methods have been validated in the EU for the safety assessment of chemicals.<sup>[17]</sup> However, none of these are as yet focused on inhalation toxicity which is highly relevant within the context of nanoparticle exposure. Furthermore, they are designed to test the hazardousness of a substance under normal physiological but not in compromised health conditions. Various ENM-specific models have been proposed as alternatives for in vivo testing but there is limited information about direct in vivo–in vitro comparisons.<sup>[18]</sup> To the best of our knowledge, no such comparisons have been carried out for in vivo versus advanced in vitro models in both healthy and diseased conditions.

In ENM-exposed mouse lung tissue or human epithelial cells, the total number of differentially expressed genes (DEG) were almost identical; 6523 and 6294 DEG in human and mouse datasets, respectively. In both human ALI and mouse models, increasing number of DEG corresponds to exposure severity (dose), and on the pathway level similar mechanisms of copper oxide nanoparticle toxicity can be found. This is in line with previous comparisons of mouse lung tissue versus submerged cultures of a human THP1 cell line exposed to carbon

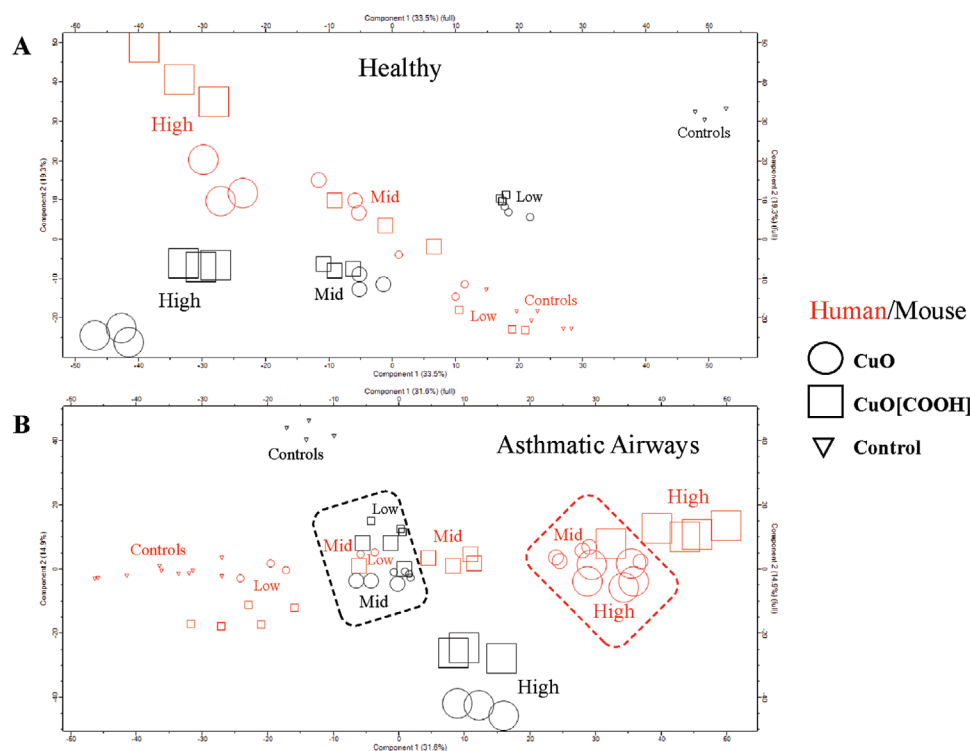


**Figure 4.** Principal component analyses of mouse–human shared differentially expressed genes in A) healthy and B) asthmatic airways exposed to pristine and COOH-functionalized copper oxide nanoparticles. Different exposures are indicated by different shapes, with circles and squares representing pristine and COOH-functionalized copper oxide nanoparticles respectively. Triangles are vehicle controls, that is, PBS for mouse lung and air for human bronchial epithelial cells cultured at the air–liquid interface. Incremental shape sizes correspond to samples exposed to different concentrations (low, mid, and high) of nanoparticles. Human samples are colored in red and mouse samples are colored black. Z-score normalization was used to scale mouse and human gene expression intensities prior to PCA analyses. In healthy airways, the top two components reveal a clear dose-response gradient in both mouse and human samples. In asthmatic airways, a dose-response variance in the gene expression can also be seen, as well as a potential disease-exposure interaction—whereby the low and mid nanoparticle concentrations cluster together in the mouse samples (black rectangle), while the mid and high nanoparticle concentrations cluster together in the human samples (red rectangle).

nanomaterials.<sup>[18]</sup> Shared mouse/human DEG were found to enrich pathways involved in responses to cytokine and toxic substances as well as oxidative stress. Incidentally, oxidative stress (in vitro) and induction of inflammation (in vivo), are the most commonly reported inhalation-relevant toxicological outcomes of exposure to copper oxide<sup>[19]</sup> and several other nanoparticles.<sup>[20]</sup>

Orthologues are genes of different species that have developed during evolution from an ancestral gene and retained the ability to encode proteins with the same function.<sup>[21,22]</sup> In order to directly compare the changes in mouse and human transcriptome, we converted mouse genes to human orthologues. Of the 18 591 mouse–human orthologue genes identified in ENSEMBL database, 15 174 were expressed in mouse lung tissue and 12 252 were commonly expressed between mouse lung tissue and human bronchial epithelial cells. Only 19% (2872 genes) of the identified orthologues were uniquely expressed in mouse lung tissue. This is a rather small fraction considering that the lung samples represent a mixture of cells such as cells of the immune system, blood vessels, connective and muscle tissue and airway epithelial cells, whilst the human ALI culture system consists only of basal, goblet, and ciliated cells that make up the bronchial epithelium. However, the anatomical proximity between the bronchioles and lungs might

explain this high degree of gene expression overlap, and supports the relevance of non-animal models that are designed as organ-level mimics. On a functional level, 1936 gene-orthologue pairs were differentially expressed in response to nanomaterial exposure in both healthy and diseased airway models, in human bronchial epithelia and mouse lung tissue. These 1936 DEG showed a very high statistically significant association (adjusted  $p$ -value up to  $10^{-57}$ ) to bronchial epithelial cells, smooth muscle, and lungs. Being that the respiratory epithelium is the front-line physical and immunological barrier to inhaled foreign bodies,<sup>[23]</sup> it is logical that the shared mouse and human DEG are highly enriched for genes that serve this purpose. Pathway analyses of the common DEG showed that the core functions of the genes triggered by nanoparticle exposure were related to responses to different stimuli covering chemicals, oxidative stress, and metal ions.

The pulmonary environment of healthy individuals and asthmatic patients displays noteworthy immunological differences. Common signs of asthma include mucus overproduction and the release of Th2-type cytokines and eosinophil-chemoattractant which induce the migration of corresponding effector cells into the lung tissue.<sup>[24]</sup> In this “pre-existing” disease state, the presence of disease-specific mediators and cells may lead to a different outcome when asthmatic

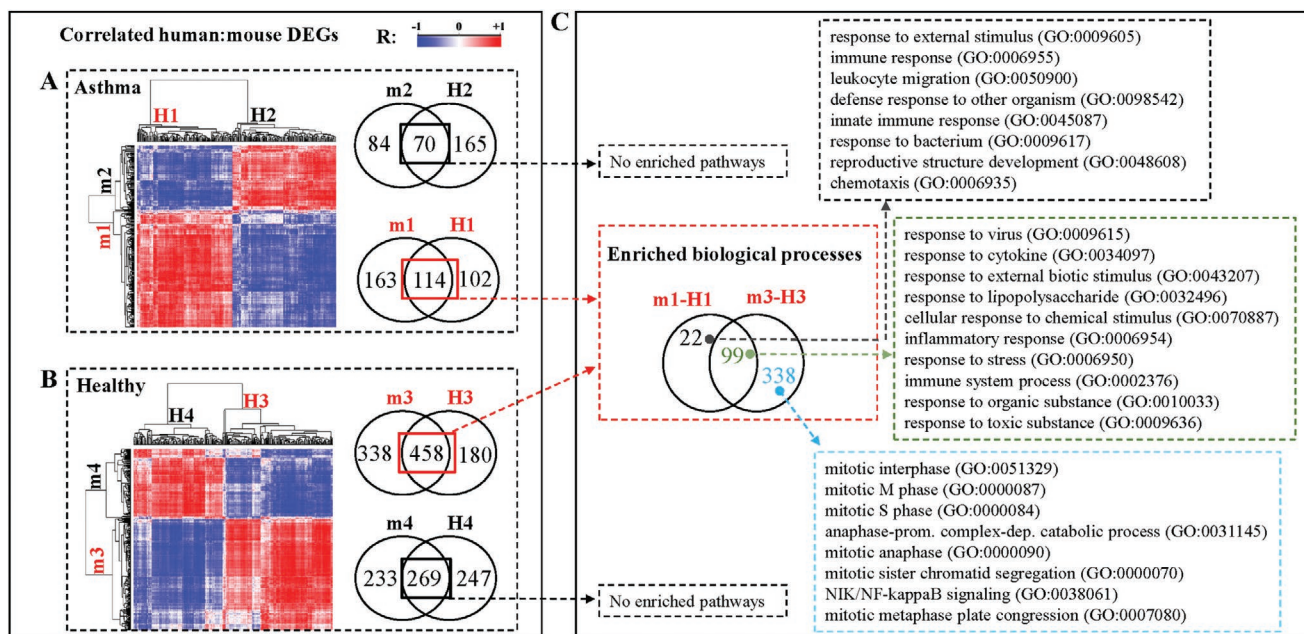


**Figure 5.** Identification of similarly activated/de-activated biological processes between shared mouse–human differentially expressed genes. Pearson’s correlation was carried out between mouse and human genes, based solely on shared differentially expressed genes in healthy or asthmatic airways. Heatmaps of highly correlated (cut-off,  $-0.8 \leq R \leq 0.8$  to at least 15 other genes) mouse–human differentially expressed genes are depicted for A) asthmatic and B) healthy airways. Clusters of positively and negatively correlated mouse–human genes were identified in shared differentially expressed genes from asthmatic and healthy airways. Clusters are named as m for mouse and H for human. Positively correlated m–H cluster pairs, that are compared with each other in the accompanying Venn diagrams, are indicated with same font colors (red: m1/H1, m3/H3 or black: m2/H2, m4/H4). Venn comparisons and gene set enrichment analyses were carried out for the positively correlated mouse–human gene clusters (A, B, right panel and C). Significantly enriched biological processes (minimum 15 genes, 5% FDR) were only identified amongst the overlapping genes shared by clusters m1–H1 (asthmatic airways) and clusters m3–H3 (healthy airways). C) A Venn comparison of all significantly enriched biological processes, as well as the top ranked biological processes are depicted. Highly positively correlated mouse–human genes were found to be involved in biological processes such as cytokine response, inflammatory response, response to toxic substance, etc. in both asthmatic and healthy airways. 22 Biological processes were unique to positively correlated mouse–human genes from asthmatic airways, with top ranked functions corresponding mainly to innate immune responses. 338 biological processes were unique to correlated mouse–human genes in healthy airways, wherein the top ranked functions were related to cell division.

airways are exposed to additional external stimuli compared to the one taking place under immunologically balanced/healthy conditions. Since asthmatics are suggested to have changes in the expression of proteins involved in innate immunity, lipid metabolism/transport, and metal ion homeostasis,<sup>[25]</sup> exposure to copper oxide particles might cause more severe effects on their health. As such, we have previously investigated healthy and asthma-type models to mechanistically unravel if and how sensitivity to ENM is altered in disease-compromised airways.<sup>[9,26]</sup> Therefore, in the current study we investigated similarities between mouse lung tissue and in vitro human ALI exposure systems, in both healthy and asthma-type models. Of the 1936 shared differentially expressed gene-orthologue pairs, 74% (1414/1893 DEG) were common to healthy mice and human epithelial cells. The number of overlapping DEG was smaller in the asthmatic setting, where only 37.6% (605/1611 DEG) of differentially expressed gene-orthologue pairs were common between mouse lung and human bronchial epithelia. Although, the shared changes of gene expression were twofold more between healthy than in the diseased airways, the number of shared enriched pathways were more alike—58% between healthy and 52% between asthmatic airways (data not shown)—confirming

that pathway-level functions are differentially conserved when compared to individual mediator genes. Forty percent of the shared mouse–human pathway-level functions enriched by the shared DEG, were found to be common between healthy and asthmatic models. As anticipated, in asthmatic airways, inflammatory responses were stronger whilst responses that were suggestive of renewal of epithelial lining (mitotic cell cycle process, spindle organization) and cilia-dependent particle clearance (microtubule-based process, cilium movement) were notably weaker. This asthma-related enhanced airway sensitivity to copper oxide ENM, is mirrored by PCA analysis based on shared differentially expressed gene-orthologue pairs. In healthy airways, a clear separation of the different concentrations of CuO and CuO<sup>COOH</sup> nanoparticles was observed, but in asthmatic airways, whilst the dose-response still exists, a narrowed range of clusters can be seen, with low and mid doses clustered together in mouse airways and mid and high doses clustered together in human bronchial epithelial cells.

Since the biological functions represented by the shared differentially expressed gene-orthologue pairs have also been previously linked to toxicity of copper oxide nanoparticles, in in vitro and in vivo systems,<sup>[9,15,27,28]</sup> we performed correlation

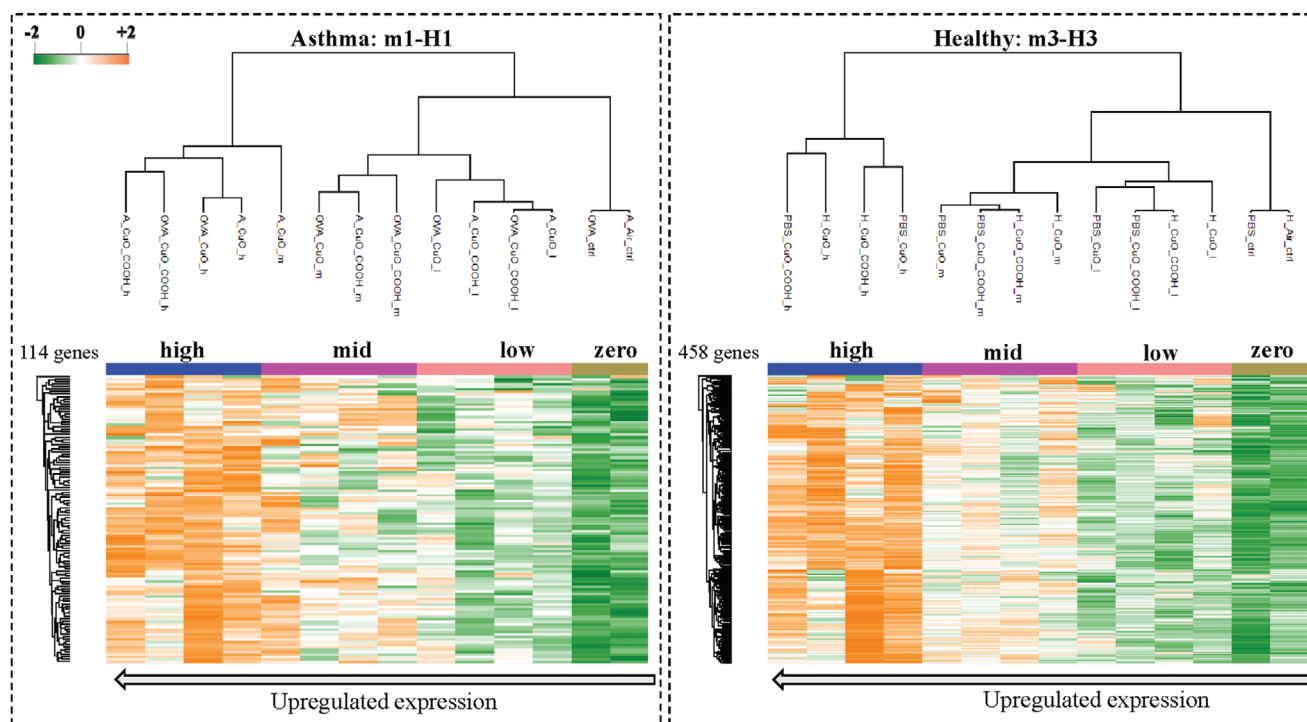


**Figure 6.** Hierarchical clustering of highly correlated mouse/human differentially expressed genes. A subset of differentially expressed genes (114 genes in asthmatic and 458 genes in healthy airways; Figure 5A,B, red boxes) common to mouse and human airways were identified as highly positively correlated, and significantly enriched for biological functions consistent with toxicant exposure (Figure 5). The expression intensities of these genes were Z-score normalized for human and mouse samples separately. Hierarchical clustering based on the normalized expression of these genes clustered samples according to nanoparticle dose—irrespective of whether samples are derived from mouse or human airways. These subsets of positively correlated mouse–human genes were mostly upregulated in response to copper oxide nanoparticles. In sample descriptions, A = asthmatic human, OVA = asthmatic mouse, H = healthy human, PBS = healthy mouse, l = low dose, m = mid dose, h = high dose, and PBS\_ctrl/OVA\_ctrl/Air\_ctrl = unexposed mouse or human samples.

analyses in tandem with functional enrichment analyses to answer whether the identified pathways were similarly activated or deactivated in mouse lung and human bronchial epithelial cells. Two pairs of highly positively correlated mouse–human gene clusters were identified, in healthy and asthmatic airways. Interestingly only one gene cluster pair in healthy and asthmatic exposure systems (m1–H1 and m3–H3) consisted of genes with enriched biological processes. These positively correlated, functionally relevant mouse–human gene-orthologue pairs were almost entirely consisting of upregulated genes

(Table S2, Supporting Information). In other words, shared downregulated mouse–human gene-orthologue pairs, though positively correlated, are not functionally interrelated and do not involve any known responses to copper oxide nanoparticles, as opposed to the shared upregulated gene-orthologue pairs. The latter are involved in inflammation, responses to various internal and external stimulants including cytokines, viruses, lipopolysaccharide and chemicals. These processes are generally associated to innate immunity, and therefore nanoparticle exposures seem to have effects on antigen presenting

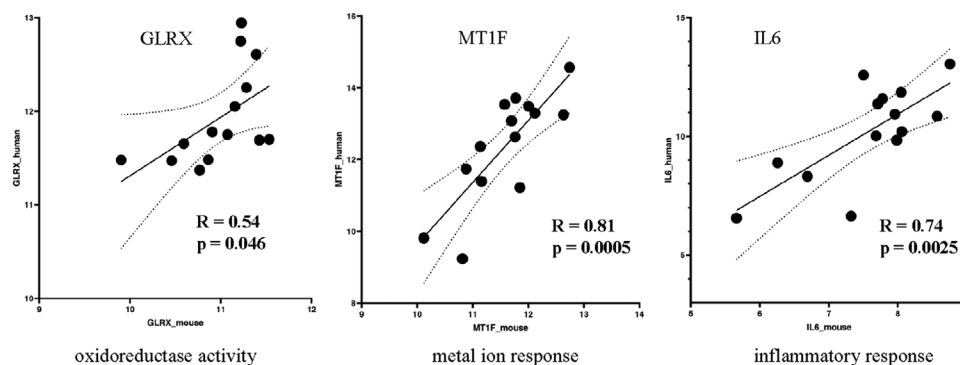


**Figure 7.** Mouse/human gene expression correlation of selected gene-orthologue pairs with functional relevance for hazardous exposure to copper oxide nanoparticles. Genes are glutaredoxin (GLRX), metallothionein 1F (MT1F) and interleukin 6 (IL6).

activities and ensuing immune responses. Since these pathways also existed in the bronchial epithelial system, it suggests that alveolar macrophages are not the only driving cell type but epithelial cells and their responses might be much more important than previously believed. Additionally, we showed that hierarchical clustering of mouse lung and human bronchial epithelial cells, based solely on the normalized expression of shared, upregulated and positively correlated mouse/human gene-orthologue pairs, incorporates the previously mentioned dose-response and enhanced airway sensitivity of asthmatic airways to nanoparticles, independent of model taxonomy, cellular complexity and particle surface charge. These genes potentially encompass a continuum of gene expression changes associated with exposure severity. As such, we propose these upregulated gene subsets as signature genes that could be assayed to evaluate diverse human and environmental exposures to copper oxide and probably other metal-based ENM.

A recurring limitation of ours and related nanotoxicological studies is the normalization of doses (or dose-related parameters) across different studies. Whilst the particle number and mass concentrations used in both the human ALI and mouse lung exposures are within the limits of feasible real-life exposures,<sup>[9,26]</sup> resolving dose effects that are independent of particle concentrations is not trivial because the different physical and chemical properties of nanoparticles, as well as the method of exposure, affect their biological and toxicological responses. Nonetheless, we are still able to identify exposure-relevant similarities at both gene and pathway levels. Most importantly, we identified a subset of upregulated genes whose relative expression in combined mouse and human samples generated clusters that were related to exposure severity, independent of the study model. Kinaret et al. previously explored the transcriptomic responses of carbon nanomaterials in the differentiated human THP-1 cell line and lung tissue of mice, and found only a small overlap of DEG but a higher similarity in enriched pathways between the human in vitro and mouse model systems.<sup>[18]</sup> This emphasizes the strength of using omics-based multi-end-point approaches in identifying even subtle similarities between models. The degree of overlap between models depends on the utilized in vitro systems—for example, human monocytic leukemia cell lines might not reflect the normal cell functioning in vivo and also submerged exposure conditions may have an effect on the outcome. 3D ALI models represent a more realistic exposure scenario, and are therefore primed to bridge the gap between traditional 2D in vitro assays and animal models. Because we identify a subset of upregulated mouse/human gene-orthologue pairs that cluster mouse and human exposures, primarily via dose, transcriptomics has the potential to be a unifying dose metric that links in vivo and in vitro test systems despite potential differences in delivered particle mass concentration, agglomeration and aggregation.

#### 4. Conclusion

We provide experimental evidence of a direct comparison of an advanced in vitro test method and its corresponding in vivo model for inhalation toxicity in the context of ENM exposure with two different model particles, at three different concentrations during healthy and compromised airway conditions. Our multiple-end-point-oriented approach based on transcriptomic

analysis showed that the traditional murine model shared a functional core of 1936 differentially expressed gene-orthologue pairs with a 3D human bronchial epithelial model. The shared genes and pathways, which we ultimately narrowed down to 114 and 458 upregulated genes in asthmatic and healthy airways, respectively, represent a potential target set of biomarkers for non-animal toxicity testing of copper oxide ENM (and related metal and metal oxide based ENM such as MnO, ZnO, TiO<sub>2</sub>, Ag, etc.) exposures, and also for the development of computational approaches for predictive hazard assessment. Extrapolating human health hazard from non-animal systems, for regulatory decision-making is complex, but these methods save time, effort, money, and are ethically more acceptable (3R principle). Our study provides knowledge that contributes to the development of non-animal testing models designed to meet specific aspects of ENM hazard assessment. The experimental and analytical approach with the obtained findings may be also useful for regulatory bodies during the validation process of alternative methods for ENM hazard assessment whose acceptance ultimately could pave a path toward the regulated use of these materials.

#### 5. Experimental Section

*Characterization of ENM:* Physicochemical characteristics of the ENM used in this study—core CuO and surface-carboxylated CuO (CuO<sup>COOH</sup>), and their behavior in different media have been reported in details earlier.<sup>[26]</sup> Preparation of ENM dispersions and generation of their aerosols has been described by Ilves et al. and Kooter et al., respectively.<sup>[9,26]</sup>

*ENM Exposures via Oropharyngeal Aspiration In Vivo:* In vivo experiments were performed in an earlier published study in which ENM were administered to mice in an ovalbumin-induced murine model of allergic airway inflammation.<sup>[26]</sup> Briefly, mice received a mixture of OVA and aluminum/magnesium hydroxide on day 1 and 10 of the sensitization period. After a 10-day recovery period, mice were exposed to saline or OVA with or without dispersed CuO materials via oropharyngeal aspiration in isoflurane anesthesia on four consecutive days. CuO materials were tested at three doses (2.5, 10, and 40 μg per mouse per administration). Mice were sacrificed 24 h after the last administration by using isoflurane overdose. Half of the left pulmonary lobe was collected after bronchoalveolar lavage for total RNA extraction and microarray analysis. Animal experiments conducted in this study were performed in agreement with the European Convention for the Protection of Vertebrate Animals Used for Experimental and Other Scientific Purposes (Strasbourg March 18, 1986, adopted in Finland May 31, 1990). All experiments were approved by the State Provincial Office of Southern Finland (ESAVI-3241-04.10.07-2013, permission number PH701A).

*ENM Aerosol Exposures at the Air-Liquid Interface In Vitro:* Details of the exposure of MucilAir 3D human airway ALI model to CuO nanoparticles have been reported previously.<sup>[9]</sup> In short, MucilAir fully differentiated bronchial epithelial cells (Epithelix Sàrl, Geneva, Switzerland) reconstituted from primary human cells of three healthy and five asthmatic donors, were exposed for 1 h in Vitrocell ALI system to clean, humidified air, low, middle, and high concentrations of CuO (23, 120, and 470 mg m<sup>-3</sup>, respectively) or CuO<sup>COOH</sup> (32, 128, and 495 mg m<sup>-3</sup>) aerosols simultaneously. Deposition rates were determined as 14% for CuO and 15% for CuO<sup>COOH</sup>, corresponding to CuO ENM doses of low (1.0 μg cm<sup>-2</sup>), mid (5.0 μg cm<sup>-2</sup>), and high (19.7 μg cm<sup>-2</sup>) and that of CuO<sup>COOH</sup> ENM being, low (1.4 μg cm<sup>-2</sup>), mid (5.8 μg cm<sup>-2</sup>), and high (22.3 μg cm<sup>-2</sup>). Cells were incubated for 24 h after the 1 h exposure and then collected for total RNA extraction and microarray analysis.

*DNA Microarrays:* Description of total RNA isolation and details on how DNA microarrays were carried out on homogenized lung or cell

lysates of 3D human bronchial epithelia ALI (MucilAir) samples, have been reported earlier.<sup>[9,26]</sup> The microarray data obtained from mouse lung samples are accessible through GEO series accession number GSE122197 and the data of human epithelial cells through the accession number GSE127773.

**Data Preprocessing, Differential Expression Analyses, and Mouse–Human Gene Sets Comparisons:** Processing of raw data and differential expression analysis were carried out separately for both data sets using eUTOPIA—a platform-independent graphical user interface based on R, with comprehensive workflows for gene expression analysis.<sup>[29]</sup> Signal intensity and background corrections were performed by quantile normalization. Batch effects due to dye and array were accounted for during differential expression analysis using the limma package.<sup>[30,31]</sup> A Benjamini–Hochberg FDR of at most 5% and abs log<sub>2</sub> difference  $\geq 0.58$  were the specified cut-offs to consider a gene as significantly different between any two contrasts. All available human orthologues for Agilent-074809 SurePrint G3 Mouse GE v2 8 × 60K Microarray were downloaded from ENSEMBL (Ensembl 98 release) genome browser using the BioMart data mining tool.<sup>[32]</sup> Where indicated, Pearson's correlation coefficient was used to investigate the relationship between commonly differentially expressed genes in mouse and human transcriptomes.

**Hierarchical Clustering and Functional Gene Set Enrichment Analysis:** The data matrix for cluster generation was quantile-normalized, and batch effects due to dye and array were adjusted with the ComBat algorithm<sup>[33]</sup> implemented in eUTOPIA. K-means based hierarchical clustering was carried out with Perseus omics analysis and visualization software.<sup>[34]</sup> To improve the separation accuracy and relevance of the generated clusters, hierarchical clustering was always performed on a specified subset of differentially expressed genes. Gene ontology based (release date 2018-04-04) identification of overrepresented biological processes were carried out using Panther enrichment analysis tool.<sup>[35]</sup> Where applicable, significantly enriched biological pathways were scored by multiplying panther-derived fold enrichment value with the  $-\log$  of the false discovery rate. Biological processes having  $<10$  genes,  $<1.5$ -fold enrichment and FDR  $\geq 0.05$  were excluded.

**Graphical Illustrations:** Bar and line plots were constructed using Prism 8 (GraphPad Software Inc., San Diego, CA, USA) or IPA software. Heat maps and PCA plots were created with Perseus, version 1.6.5.0.<sup>[36]</sup> and Venn comparisons were done with Venny 2.1.0.<sup>[37]</sup>

## Supporting Information

Supporting Information is available from the Wiley Online Library or from the author.

## Acknowledgements

J.N. and M.I. contributed equally to this work. The authors thank the Seventh Framework Programme (grant number 309329) and the Academy of Finland (grant numbers 297885 and 307768) for funding.

## Conflict of Interest

The authors declare no conflict of interest.

## Keywords

air–liquid interface, copper oxide nanoparticles, mouse versus human, nanosafety, non-animal, transcriptomics

Received: January 27, 2020

Revised: March 23, 2020

Published online:

- [1] M. E. Andersen, D. Krewski, *Toxicol. Sci.* **2009**, *107*, 324.
- [2] N. Burden, K. Aschberger, Q. Chaudhry, M. J. D. Clift, S. H. Doak, P. Fowler, H. Johnston, R. Landsiedel, J. Rowland, V. Stone, *Nano Today* **2017**, *12*, 10.
- [3] T. A. Stueckle, J. R. Roberts, *Appl. In Vitro Toxicol.* **2019**, *5*, 111.
- [4] I. M. Kooter, M. Gröllers-Mulderij, M. Steenhof, E. Duistermaat, F. A. A. van Acker, Y. C. M. Staal, P. C. Tromp, E. Schoen, C. F. Kuper, E. van Someren, *Appl. In Vitro Toxicol.* **2016**, *2*, 56.
- [5] P. S. Hiemstra, G. Grootaers, A. M. van der Does, C. A. M. Krul, I. M. Kooter, *Toxicol. In Vitro* **2018**, *47*, 137.
- [6] S. Huang, M. Caulfuty, *A Novel In Vitro Cell Model of the Human Airway Epithelium*, 3R-Info-Bulletin, Münsingen, Switzerland **2009**.
- [7] M. Lundqvist, J. Stigler, T. Cedervall, T. Berggård, M. B. Flanagan, I. Lynch, G. Elia, K. Dawson, *ACS Nano* **2011**, *5*, 7503.
- [8] S. G. Klein, T. Serchi, L. Hoffmann, B. Blömeke, A. C. Gutleb, *Part. Fibre Toxicol.* **2013**, *10*, 31.
- [9] I. Kooter, M. Ilves, M. Gröllers-Mulderij, E. Duistermaat, P. C. Tromp, F. Kuper, P. Kinaret, K. Savolainen, D. Greco, P. Karisola, *ACS Nano* **2019**, *13*, 6932.
- [10] B. Fadeel, L. Farcas, B. Hardy, S. Vázquez-Campos, D. Hristozov, A. Marcomini, I. Lynch, E. Valsami-Jones, H. Alenius, K. Savolainen, *Nat. Nanotechnol.* **2018**, *13*, 537.
- [11] G. K. Andrews, *Biochem. Pharmacol.* **2000**, *59*, 95.
- [12] A. Nagy, J. A. Hollingsworth, B. Hu, A. Steinbrück, P. C. Stark, C. Rios Valdez, M. Vuyisich, M. H. Stewart, D. H. Atha, B. C. Nelson, R. Iyer, *ACS Nano* **2013**, *7*, 8397.
- [13] H. J. Eom, N. Chatterjee, J. Lee, J. Choi, *Toxicol. Lett.* **2014**, *229*, 311.
- [14] L. Peng, M. He, B. Chen, Y. Qiao, B. Hu, *ACS Nano* **2015**, *9*, 10324.
- [15] W.-L. Poon, H. Alenius, J. Ndika, V. Fortino, V. Kolhinen, A. Meščeriakovas, M. Wang, D. Greco, A. Lähde, J. Jokiniemi, J. C.-Y. Lee, H. El-Nezami, P. Karisola, *Nanotoxicology* **2017**, *11*, 936.
- [16] J. Ndika, U. Seemab, W.-L. Poon, V. Fortino, H. El-Nezami, P. Karisola, H. Alenius, *Nanotoxicology* **2019**, *13*, 1380.
- [17] V. Zuang, A. Dura, D. Asturiel Bofill, J. Barroso, S. Batista Leite, S. Belz, E. Berggren, C. Bernasconi, S. Bopp, M. Bouhifd, G. Bowe, I. Campia, S. Casati, S. Coecke, R. Corvi, L. Gribaldo, E. Grignard, M. Halder, M. Holloway, A. Kienzler, B. Landesmann, F. Madia, A. Milcamps, S. Morath, S. Munn, A. Paini, F. Pistollato, A. Price, M. Prieto Peraita, A. Richarz, J. Sala Benito, I. Wilk-Zasadna, C. Wittwehr, A. Worth, M. Whelan, *EURL ECVAM Status Report on the Development, Validation and Regulatory Acceptance of Alternative Methods and Approaches*, Publications Office of the European Union, Brussels, Belgium **2018**.
- [18] P. Kinaret, V. Marwah, V. Fortino, M. Ilves, H. Wolff, L. Ruokolainen, P. Auvinen, K. Savolainen, H. Alenius, D. Greco, *ACS Nano* **2017**, *11*, 3786.
- [19] M. Ahamed, M. J. Akhtar, H. A. Alhadlaq, S. A. Alrokayan, *Nano-medicine* **2015**, *10*, 2365.
- [20] S. Bakand, A. Hayes, F. Dechsakulthorn, *Inhalation Toxicol.* **2012**, *24*, 125.
- [21] W. M. Fitch, *Syst. Zool.* **1970**, *19*, 99.
- [22] B. Georgi, B. F. Voight, M. Bučan, *PLoS Genet.* **2013**, *9*, e1003484.
- [23] P. S. Hiemstra, P. B. McCray, R. Bals, *Eur. Respir. J.* **2015**, *45*, 1150.
- [24] M. Caminati, D. Le Pham, D. Bagnasco, G. W. Canonica, *World Allergy Organ. J.* **2018**, *11*, 13.
- [25] A. Kumar, E. M. Bicer, P. Pfeffer, M. P. Monopoli, K. A. Dawson, J. Eriksson, K. Edwards, S. Lynham, M. Arno, A. F. Behndig, A. Blomberg, G. Somers, D. Hassall, L. A. Dailey, B. Forbes, I. Mudway, *Nanomedicine* **2017**, *13*, 2517.
- [26] M. Ilves, P. A. S. Kinaret, J. Ndika, P. Karisola, V. Marwah, V. Fortino, Y. Fedutik, M. Correia, N. Ehrlich, K. Loeschner, *Part. Fibre Toxicol.* **2019**, *16*, 28.
- [27] N. Hanagata, F. Zhuang, S. Connolly, J. Li, N. Ogawa, M. Xu, *ACS Nano* **2011**, *5*, 9326.

- [28] P. M. Costa, I. Gosens, A. Williams, L. Farcas, D. Pantano, D. M. Brown, V. Stone, F. R. Cassee, S. Halappanavar, B. Fadeel, *J. Appl. Toxicol.* **2017**, 385.
- [29] V. S. Marwah, G. Scala, P. A. S. Kinaret, A. Serra, H. Alenius, V. Fortino, D. Greco, *Source Code Biol. Med.* **2019**, 14, 1.
- [30] G. K. Smyth, in *Bioinformatics and Computational Biology Solutions Using R and Bioconductor*, Springer, Berlin **2005**, pp. 397–420.
- [31] M. E. Ritchie, B. Phipson, D. Wu, Y. Hu, C. W. Law, W. Shi, G. K. Smyth, *Nucleic Acids Res.* **2015**, 43, e47.
- [32] F. Cunningham, P. Achuthan, W. Akanni, J. Allen, M. R. Amode, I. M. Armean, R. Bennett, J. Bhai, K. Billis, S. Boddu, C. Cummins, C. Davidson, K. J. Dodiya, A. Gall, C. G. Girón, L. Gil, T. Grego, L. Haggerty, E. Haskell, T. Hourlier, O. G. Izuogu, S. H. Janacek, T. Juettemann, M. Kay, M. R. Laird, I. Lavidas, Z. Liu, J. E. Loveland, J. C. Marugán, T. Maurel, *Nucleic Acids Res.* **2019**, 47, D745.
- [33] J. T. Leek, W. E. Johnson, H. S. Parker, A. E. Jaffe, J. D. Storey, *Bioinformatics* **2012**, 28, 882.
- [34] S. Tyanova, T. Temu, P. Sinitcyn, A. Carlson, M. Y. Hein, T. Geiger, M. Mann, J. Cox, *Nat. Methods* **2016**, 13, 731.
- [35] H. Mi, X. Huang, A. Muruganujan, H. Tang, C. Mills, D. Kang, P. D. Thomas, *Nucleic Acids Res.* **2017**, 45, D183.
- [36] S. Tyanova, T. Temu, P. Sinitcyn, A. Carlson, M. Y. Hein, T. Geiger, M. Mann, J. Cox, *Nat. Methods* **2016**, 13, 731.
- [37] J. C. Oliveros, (2007–2015) VENNY. An Interactive Tool for Comparing Lists with Venn Diagrams, <http://bioinfogp.cnb.csic.es/tools/venny/index.html> (accessed: December 2019).